ARMA 23–0562

Numerical investigation of mining-induced, hydromechanically-coupled responses for a Nevada mine site

Noonan, G.E.
Geotechnical Center of Excellence - University of Arizona, Tucson, Arizona, USA
Lorig, L.J.
Itasca Consulting Group, Inc., Minneapolis, MN, USA
Beale, G.
Piteau Associates, Shrewsbury, UK
Ferré, P.A.
University of Arizona, Tucson, Arizona, USA

This paper was prepared for presentation at the 57th US Rock Mechanics/Geomechanics Symposium held in Atlanta, Georgia, USA, 25-28 June 2023. This paper was selected for presentation at the symposium by an ARMA Technical Program Committee based on a technical and critical review of the paper by a minimum of two technical reviewers. The material, as presented, does not necessarily reflect any position of ARMA, its officers, or members. Electronic reproduction, distribution, or storage of any part of this paper for commercial purposes without the written consent of ARMA is prohibited. Permission to reproduce in print is restricted to an abstract of not more than 200 words; illustrations may not be copied. The abstract must contain conspicuous acknowledgement of where and by whom the paper was presented.

ABSTRACT: Understanding the coupled interaction of rock and water under stress is often a key factor in assessing slope stability in open pit mining. In this paper, a numerical modeling research project is presented which demonstrates the concept of hydromechanical coupling (HMC) and assesses the sensitivity of contributing parameters to pressure responses observed in a piezometer sensor due to excavation of a mine slope. Site monitoring data showing HMC effects within a mine in Nevada are analyzed and reproduced using *FLAC*. This research aims to promote the understanding of HMC in pit slopes and provide improved guidance on how to plan mining activity, monitoring and slope design to incorporate the benefit of HMC effects.

1. INTRODUCTION

Open-pit mining is a dynamic process that involves the excavation of earth materials to retrieve ore. During the mining process, changes to the physical properties of the in-situ rock mass are induced. As excavations progress, pore pressure changes occur beyond the slope face, and, while some factors such as infiltration or recharge may increase the pore pressure, others may help reduce it. Consequently, understanding the relation between pore pressure changes and rock deformation is a key factor in ensuring the stability of slopes and maintaining safe mining conditions. Pore pressure can be measured, predicted, and managed through active dewatering and depressurization programs to control stability.

In this research paper, 2D modeling using *FLAC* v8.1 is presented to help explain observed behaviors in piezometer monitoring data from a mine site in Nevada, and to provide a hydromechanical explanation for these behaviors using simple model illustrations. Different case scenarios using a variation of mechanical and hydrological input parameters are performed. Varied parameters are those which govern pore pressure responses caused by induced changes in total effective stress (unloading) of the rock mass, such as elastic modulus, porosity, and permeability. Results are presented and discussed for each modeling case scenario using pore pressure history at a point representing the piezometer sensor location.

2. THEORY

Hydromechanical coupling is the interaction between hydraulic and mechanical processes. The benefit of understanding these coupled processes in the design and operation of mine slopes has been presented in detail by Beale (2018), Beale and Read (2014), and Sullivan (2007).

These processes are comprised in Terzaghi's concept of effective stress (Terzaghi, 1943) which is a fundamental principle in open pit rock slope design. Terzaghi's Principle states that when stress is applied to a porous material, it is opposed by the fluid pressure filling the pores in the material. Both shear strength and deformation are controlled by effective stress. Fluid pressure acts to reduce the effective normal stress on a surface, contributing to slope failure mechanisms. Excavation of a slope, via removal of overburden or blasting, causes changes in rock stress which will in turn affect fluid pressures.

Using Terzaghi's Principle, the vertical effective stress (σ_v') is equal to the vertical total stress (σ_v), minus the pressure in the pores or joints (μ). The most common form for the effective stress law is:

$$\sigma_{v'} = \sigma_v - \mu \qquad (1)$$

When a mechanical change occurs, the pore pressure changes according to Skempton's coefficient (B):

$$B = \frac{\Delta p}{\Delta \sigma} = \frac{\Delta p}{\Delta p + \Delta \sigma'} = \frac{\frac{K_w}{n}}{\left(\frac{K_w}{n}\right) + K} \qquad (2)$$

Where $\Delta\rho$ = pore pressure change, $\Delta\sigma$ = change in mean total stress, $\Delta\sigma$' = change in mean effective stress, K_w = water bulk modulus, n = porosity, and K = rock bulk modulus.

The poroelastic response of soil and rock can be visualized using Figure 1, where the relation of K and K_w/n are shown to correspond to changes in total stress ($\Delta\sigma$) during unloading.

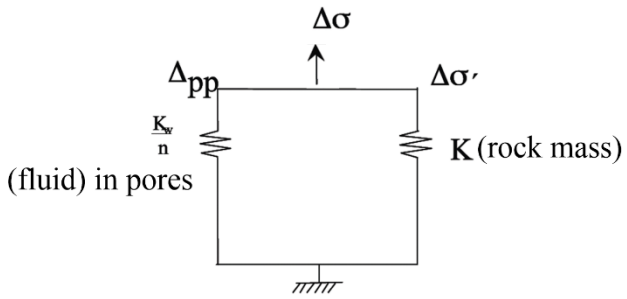

Fig. 1. Poroelastic stress distribution (modified from Galera et al., 2009).

3. CONCEPTUALIZATION

The modeling presented in this paper is based on observations of piezometer data from a mine site in Nevada with a given sequence of mine excavations (Figure 2). It can be seen that the observed piezometric levels drop due to stress relief occurring in correlation with the removal of material (mining excavation). Following these piezometric drops, gradual recovery can be observed; however, full recovery back to starting levels does not occur. The pore pressure measured by the piezometer is directly related to the water level height in the piezometer (h) through the following equation:

$$\mu = \gamma_w h \qquad (3)$$

where (γ_w) is the unit weight of water.

Our modeling aims to recreate a simplified and generalized version of the given mine site geology and geometry to look at reproducing similar pore pressure responses via coupled hydromechanical model manipulation.

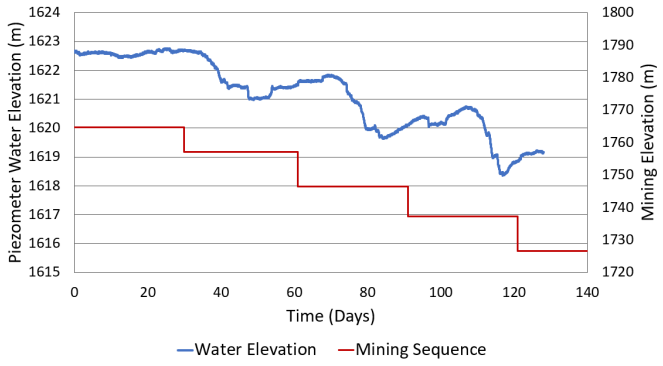

Fig. 2. Mine site piezometer (water elevation (blue) on left axis) and mining sequence (mining elevation (red) on right axis) data versus time (days).

4. NUMERICAL MODEL

A simplified and generalized numerical model was created to examine a sequence of three excavation increments of the slope and assess the effect of these excavations on modeled pore pressure. The material in the slope is assumed to behave elastically. As is common practice, the model represents the rock as an equivalent porous medium (EPM) and assumes that fractures are closely spaced relative to the scale of the slope.

The model was created with the two-dimensional finite difference program *FLAC*. Similar analyses have been performed and described by Galera et al. (2009) and Hazzard et al. (2011) to test different *FLAC* modeling procedures under different mechanical and hydraulic conditions. In this model we use a simple two-way coupled (undrained-drained) approach. The simplified two-way coupling involves an undrained mechanical analysis (short-time response) followed by one-way coupling with groundwater flow (transient response). This approach assumes that pressure changes due to pit-slope excavation occur more-or-less instantaneously and that flow can be ignored in the short-term during the mechanical analysis.

In this analysis, the mine site is represented by a simplified three-layer stratigraphy consisting of alluvium overlying sandstone, with tuff below (Figure 3). The units and their properties are well constrained based on the geological profile and geotechnical data provided by the mine. Layer thicknesses and orientations are simplified, and minor geological units are omitted, as is structure (faulting). A phreatic surface is included that initially lies in the alluvium unit at a height of 250 m above the base of the model.

A history point, located generally where the site piezometer sensor is placed within the central sandstone unit, is included in the model to track the pore pressure responses versus flow time, for each model case scenario.

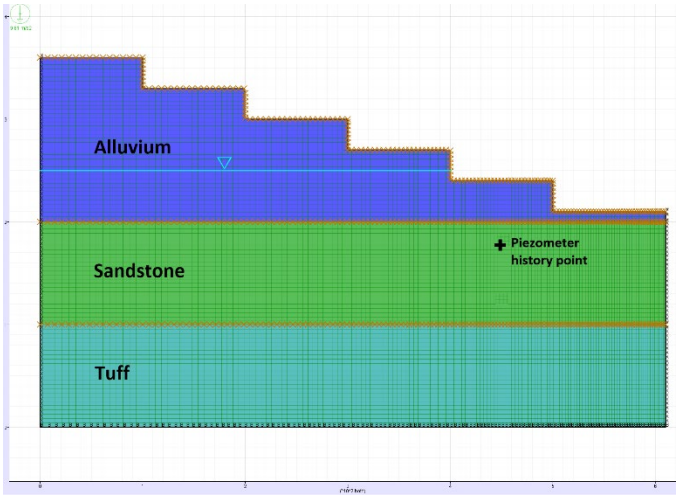

Fig. 3. *FLAC* model representing generalized mine site geology and geometry.

Figure 4 shows the excavation sequence for the modeling, which approximates the actual mining sequence in size, distance from the piezometer, and timing. The excavations occur approximately one month apart.

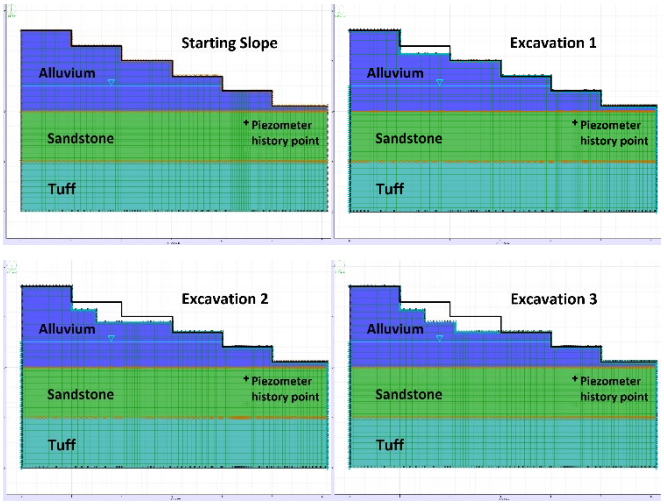

Fig. 4. Excavation sequence used in modeling (three excavation increments, both to the left and above the piezometer location).

The boundary conditions for the mechanical problem are fixed in the x direction on the left- and right-hand boundaries, and in the x and y direction at the bottom of the model. Initial stress conditions represent loading due to gravity, and the ratio of horizontal-to-vertical stress is one.

At the left-hand side of the model, a constant pressure head is applied to represent the height of the phreatic surface. On the right-hand side, this pressure head reflects the height of the toe of the slope in the model space, and there is a no-flow boundary at the base. A zero (atmospheric) pore pressure is assigned to the slope face. In *FLAC*, for a single-phase-fluid model and flow in which a phreatic surface develops, pore pressures are zero above the phreatic surface and the air phase is considered to be passive. For a free surface (i.e., at the top of the model), the boundary is based on *FLAC*'s assumption, using the single-phase option, that pore pressures can only exist in a fully saturated material (Itasca Consulting Group, Inc., 2019).

Initially, the model is in static equilibrium and flow is simulated for 90 days (or more) to achieve steady- or near-steady state conditions. In the undrained portion of the analysis, a mechanical solution is simulated without flow i.e., fluid flow calculations are turned off, and mechanical calculations are turned on. Each mechanical excavation occurs instantaneously. The drained analysis then is run by turning the flow calculation on and turning the mechanical calculation off and the flow is simulated for 30 days. Transient pore pressures are obtained and plotted versus flow time.

Rock and fluid properties given by the mine and used in the starting model (Model Case A) are shown in Table 1. It should be noted that:

- The bulk and shear modulus values represent average values from a provided range for each unit.
- Specific yield (or drainable porosity) is used as a proxy for porosity in the model input (specific yield is less than porosity since some water will be retained in the aquifer by molecular and surface tension). In this paper, porosity refers to drainable porosity.
- Surface infiltration was not considered in this analysis, nor were other induced hydraulic effects from pumping or drains.
- A homogeneous anisotropic permeability is assumed for each unit.
- *FLAC* input uses the intrinsic permeability (κ); the relationship between the intrinsic permeability and the hydraulic conductivity (k) is given by:

$$\kappa = \left(\frac{k}{g\rho_w}\right) \qquad (4)$$

  with gravity (g), and water density (ρ_w).
- Parameters studied in the combined analyses were considered independently and are not linked to each other, whereas in reality they may be dependent.

The results of the starting model for the three representative excavations are shown in Figure 5 (pore pressure at the piezometer history point versus groundwater flow time). It can be observed that, when the material is excavated, there is a pore-pressure drop to zero, indicating the material in the vicinity of the piezometer has quickly lost pressure. The duration of this pressure drop is represented in the time series plot as

instantaneous due to the simplified two-way coupling approach; in this approach, flow is turned off during the mechanical step and thus there is zero 'flow time' associated with the excavation. As flow is again introduced, the pore pressure recovers very quickly, but with each resulting excavation, the pore pressure again drops to zero. Stress relief due to the excavations is producing rapid drops in pore pressure in this model case scenario.

Table 1. Given rock and fluid properties for Model Case A (starting model).

Property	Unit	Value
Fluid density, ρ_w	All	997 kg/m^3
Fluid bulk modulus, K_w	All	2.1E8 Pa
Bulk modulus, K	Alluvium	4.40E+08 Pa
	Sandstone	1.05E+09 Pa
	Tuff	5.67E+09 Pa
Shear modulus, G	Alluvium	2.05E+08 Pa
	Sandstone	4.85E+08 Pa
	Tuff	3.41E+09 Pa
Specific yield, Sy	Alluvium	0.2
	Sandstone	0.0025
	Tuff	0.005
Density, ρ	Alluvium	2060 kg/m^3
	Sandstone	1990 kg/m^3
	Tuff	2430 kg/m^3
Horizontal permeability, k_{11}	Alluvium	1.02E-11 m^2
	Sandstone	1.02E-08 m^2
	Tuff	1.02E-09 m^2
Vertical permeability, k_{22}	Alluvium	1.02E-11 m^2
	Sandstone	1.02E-12 m^2
	Tuff	1.02E-09 m^2

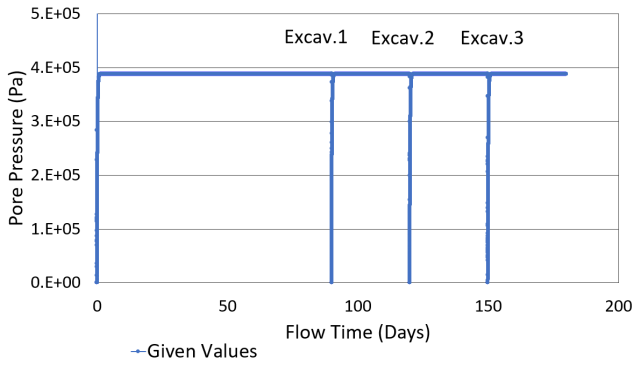

Fig. 5. Modeled pore pressure (Pa) versus groundwater flow time (days) for Model Case A.

The modeled hydromechanical behavior depends on multiple parameters, including the bulk and shear modulus (which describe the stiffness of the rock), porosity (drives storage capacity of the material), and permeability (governs ease of flow through the material, and therefore, recovery time). To assess the impact of each of these governing parameters, they are varied and run as both separate and combined model analyses. The results of these varied cases are presented in Section 4.2 and are summarized in Table 2.

Table 2. Modified rock and fluid properties for varied cases.

Model	Parameter Variation
Case A	Given site parameters
Case B	Increase bulk/shear moduli of all units
Case C	Increase porosity of sandstone unit
Case D	Decrease k_{11} of sandstone unit
Case E	Decrease k_{22} of sandstone unit
Case F	Increase porosity of sandstone unit, increase bulk/shear moduli of all units
Case G	Increase porosity of sandstone unit, decrease k_{11} of sandstone
Case H	Increase porosity of sandstone unit, decrease k_{11} of sandstone, increase bulk/shear moduli of all units

4.1. Model Verification

Mechanical volume changes are associated with changes in pore pressure (i.e., volumetric expansion of a rock mass enables a corresponding drop in pore pressure).

The Biot coefficient for porous rock (α) is a scalar quantity (between 0 and 1) that relates how compressible a rock mass is compared to the intact rock, and plays a significant role in the volumetric behavior of the rock as described by the volumetric stress-strain equation:

$$\sigma - \alpha p = K\varepsilon \qquad (5)$$

where σ is the mean total stress, ρ is fluid pressure, K is the rock-mass bulk modulus, and ε is volumetric strain.

If the Biot coefficient is assumed equal to 1 (i.e., intact rock blocks are rigid relative to the rock mass), we can calculate the change in pore pressure (Δp) given a change in volumetric strain (Δε), the bulk modulus of water (K_w), and the porosity (n) by:

$$\Delta p = K_w * \left(\frac{\Delta\varepsilon}{n}\right) \qquad (6)$$

To verify the behavior of our best-fitting model, Equation 6 was used to calculate the expected pore pressure change based on the modeled volumetric strain for each excavation stage (Excavation 1, 2 and 3) for Model Case H; all sequences demonstrated less than 5% difference of predicted pore pressure change based on modeled volumetric strain.

4.2. Mechanical /Fluid-Flow Parameter Variation

A series of models were run using the base-case scenario (Model Case A) and varying mechanical and hydrological parameters such as the bulk and shear moduli of all units, and the porosity and permeability of the rock hosting the piezometer (sandstone). As previously discussed, in the stress/strain relation, stiffness of the rock mass and porosity are related to the change in total stress, in our case caused by unloading of the slope. The recovery of the pore pressures with the reintroduction of flow relies

on porosity and permeability, and the rate at which pore pressure dissipates depends on porosity, fluid bulk modulus and rock stiffness.

Model Case B:

In an attempt to reduce the rapid and complete pore pressure drop that occurred in the base-case scenario model with the unloading events, and to assess the sensitivity of the bulk and shear moduli to the pore pressure response, the bulk and shear moduli of all three unit layers (alluvium, sandstone, and tuff) were increased by one order-of-magnitude. The modified rock and fluid properties used in Model Case B are provided in Table 3.

Table 3. Modified rock and fluid properties for Model Case B.

Property	Unit	Value
Bulk modulus, K	Alluvium	4.40E+09 Pa
	Sandstone	1.05E+10 Pa
	Tuff	5.67E+10 Pa
Shear modulus, G	Alluvium	2.05E+09 Pa
	Sandstone	4.85E+09 Pa
	Tuff	3.41E+10 Pa

Modeled pressures versus groundwater flow time for Model Case B are presented in Figure 6. It can be observed that the pore pressures following each excavation no longer plummet to zero, indicating that increasing the stiffness of the material allows the slope to retain more realistic starting pressures prior to initiation of the drained analysis stage. The model also approaches the initial solved equilibrium flow state over a shorter period of time than with the starting parameter scenario. The recovery to starting pore pressure is again nearly immediate in Model Case B with the re-initiation of flow into the model following excavation stages.

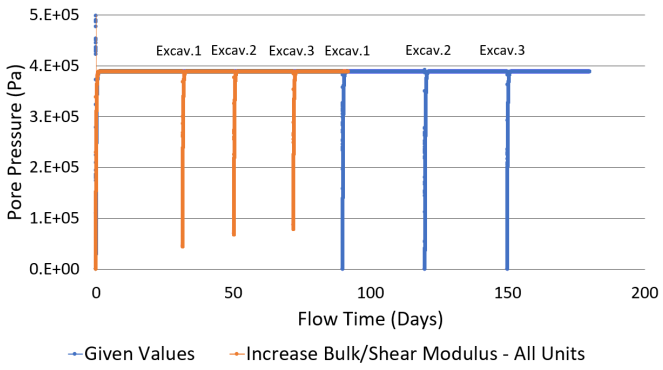

Fig. 6. Modeled pore pressure (Pa) versus groundwater flow time (days) for Model Case B (orange) and Model Case A (blue).

Model Case C:

Also in an attempt to further limit the rapid pore pressure drop that occurred in the base-case scenario model with unloading, and to assess the sensitivity of the porosity to the pore pressure response, in Model Case C, the porosity of the sandstone unit was increased by one order-of-magnitude. The modified rock and fluid properties used in Model Case C are provided in Table 4.

Table 4. Modified rock and fluid properties for Model Case C.

Property	Unit	Value
Porosity	Sandstone	0.025

Modeled pressures versus groundwater flow time for Model Case C are presented in Figure 7. Similar to Model Case B, it can be observed that the pore pressures following each excavation no longer go to zero, indicating that increasing the porosity of the material allows the slope to retain more realistic starting pressures prior to initiation of each drained analysis stage. The model also shows a more gradual recovery to starting pore pressures with initiation of flow into the model following each excavation.

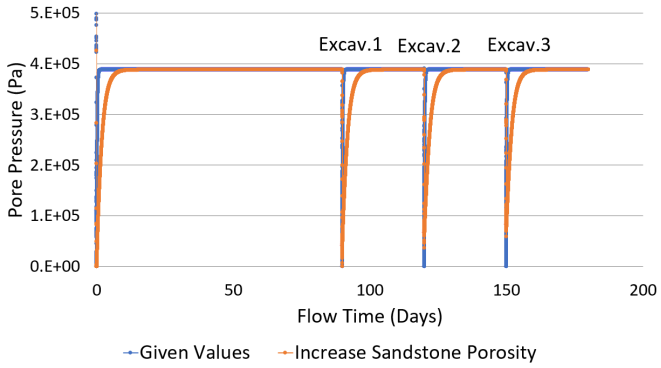

Fig. 7. Modeled pore pressure (Pa) versus groundwater flow time (days) for Model Case C (orange) and Model Case A (blue).

Model Case D:

The permeability of the material will affect pore pressure recovery time as it controls the rate of flow. Model Case D attempts to reduce the speed of the pore pressure recovery that occurs in previous scenario models during the drained analysis, and to assess the sensitivity of the horizontal permeability to the modeled pore pressure response. This case-scenario decreases the horizontal permeability of the sandstone unit by one order-of-magnitude. The modified rock and fluid properties used in Model Case D are provided in Table 5.

Table 5. Modified rock and fluid properties for Model Case D.

Property	Unit	Value
Horizontal permeability, k_{11}	Sandstone	1.02E-09 m^2

Modeled pressures versus groundwater flow time for Model Case D are presented in Figure 8. Similar to Model Case C (where the porosity of the sandstone was increased), it can be observed that Model Case D also shows a more gradual recovery to starting pore pressures with initiation of flow into the model following each

excavation; however, pore pressures following each excavation again go to zero, indicating that the model is draining during each mechanical excavation stage. It should also be noted that the initial flow stage to equilibrium no longer reaches the steady-state starting pressure within a 90-day flow interval; hence, for reduced-permeability analyses, the initializing flow should be extended longer over time to reach steady-state starting conditions.

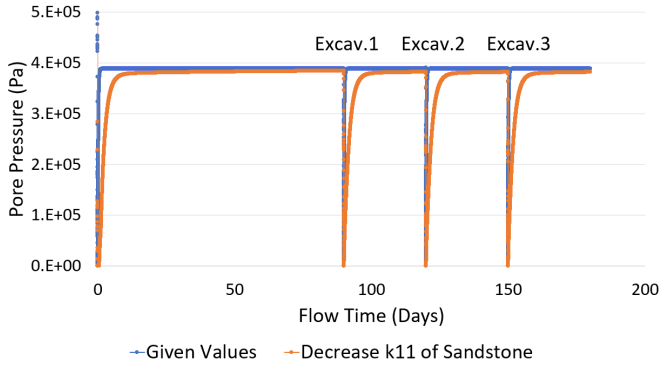

Fig. 8. Modeled pore pressure (Pa) versus groundwater flow time (days) for Model Case D (orange) and Model Case A (blue).

Model Case E:

Model Case E assesses the sensitivity of the vertical permeability to the pore pressure response. This case-scenario decreases the vertical permeability of the sandstone unit by one order-of-magnitude. The modified rock and fluid properties used in Model Case E are provided in Table 6.

Table 6. Modified rock and fluid properties for Model Case E.

Property	Unit	Value
Vertical permeability, k_{22}	Sandstone	1.02E-13 m^2

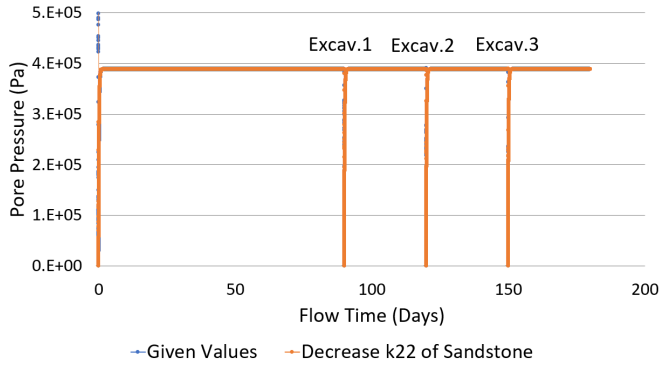

Fig. 9. Modeled pore pressure (Pa) versus groundwater flow time (days) for Model Case E (orange) and Model Case A (blue).

Modeled pressures versus groundwater flow time for Model Case E are presented in Figure 9. Decreasing the vertical permeability for the sandstone unit produced little to no change in the modeled pore pressures from the base-case scenario.

Model Case F:

Model Case F combines two previous cases to assess both increasing the porosity of the sandstone unit and increasing the bulk/shear moduli of all units by one order-of-magnitude. The modified rock and fluid properties used in Model Case E are provided in Table 7.

Table 7. Modified rock and fluid properties for Model Case F.

Property	Unit	Value
Bulk modulus, K	Alluvium	4.40E+09 Pa
	Sandstone	1.05E+10 Pa
	Tuff	5.67E+10 Pa
Shear modulus, G	Alluvium	2.05E+09 Pa
	Sandstone	4.85E+09 Pa
	Tuff	3.41E+10 Pa
Porosity	Sandstone	0.025

Modeled pressures versus groundwater flow time for Model Case F are presented in Figure 10. With the combination of increased porosity of the sandstone and increased stiffness of all units in the model, the effect on pore pressure behavior includes a quicker approach to initial flow equilibrium, as well as a higher retained pore pressure as a starting point following each excavation stage. Again, the pressure returns to previous pore pressure values within the 30-day flow recovery window, though more gradually than in the base-case scenario.

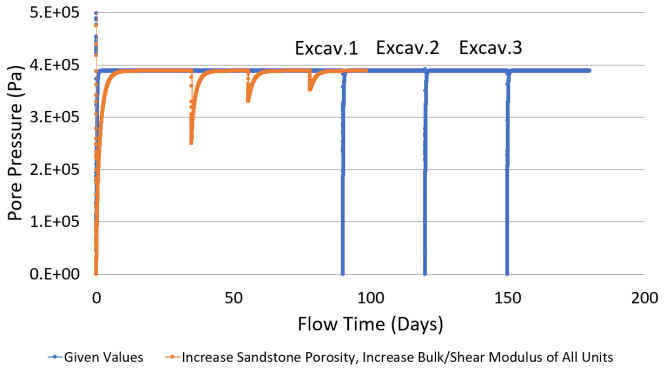

Fig. 10. Modeled pore pressure (Pa) versus groundwater flow time (days) for Model Case F (orange) and Model Case A (blue).

Model Case G:

Model Case G combines two previous cases to assess both increasing the porosity of the sandstone unit and decreasing k_{11} of the sandstone, both by one order-of-magnitude. The modified rock and fluid properties used in Model Case G are provided in Table 8.

Modeled pressures versus groundwater flow time for Model Case G are presented in Figure 11. Based on the results of Model Case D, where the decrease in

permeability showed that a longer initial flow time to reach equilibrium was required, this model was run initially to contain significant extended flow time prior to the first excavation. Increasing the porosity of the sandstone allows higher (more realistic) starting pressures following each excavation as the material retains water more readily. The combined increase in porosity and decrease in permeability of the sandstone deters the model from reaching full recovery to pre-excavation pore pressure magnitudes for each excavation stage.

Table 8. Modified rock and fluid properties for Model Case G.

Property	Unit	Value
Porosity	Sandstone	0.025
Horizontal permeability, k_{11}	Sandstone	1.02E-09 m^2

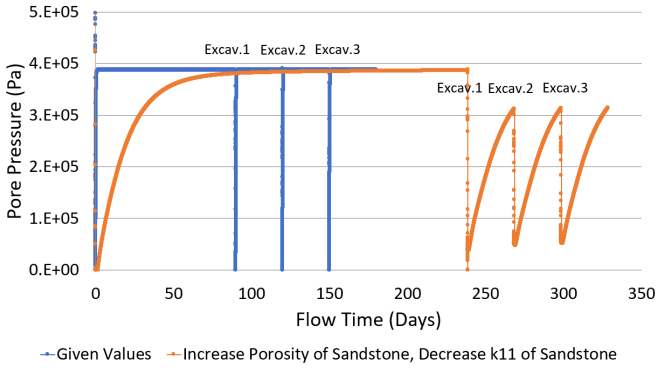

Fig. 11. Modeled pore pressure (Pa) versus groundwater flow time (days) for Model Case G (orange) and Model Case A (blue).

Model Case H:

The final model case, Model Case H, combines three previous cases to assess increased porosity of the sandstone unit, decreased k_{11} of sandstone, and increased bulk/shear modulus of all units, all varied by one order-of-magnitude. The modified rock and fluid properties used in Model Case H are provided in Table 9.

Table 9. Modified rock and fluid properties for Model Case H.

Property	Unit	Value
Bulk modulus, K	Alluvium	4.40E+09 Pa
	Sandstone	1.05E+10 Pa
	Tuff	5.67E+10 Pa
Shear modulus, G	Alluvium	2.05E+09 Pa
	Sandstone	4.85E+09 Pa
	Tuff	3.41E+10 Pa
Porosity	Sandstone	0.025
Horizontal permeability, k_{11}	Sandstone	1.02E-09 m^2

Modeled pressures versus groundwater flow time for Model Case H are presented in Figure 12. A combination of increased porosity of sandstone, increased bulk/shear modulus of all units, and decreased horizontal permeability of the sandstone results in increased pore pressure retainment with each excavation, and delayed recovery to starting pore pressures with each excavation due to the decreased permeability in the sandstone unit.

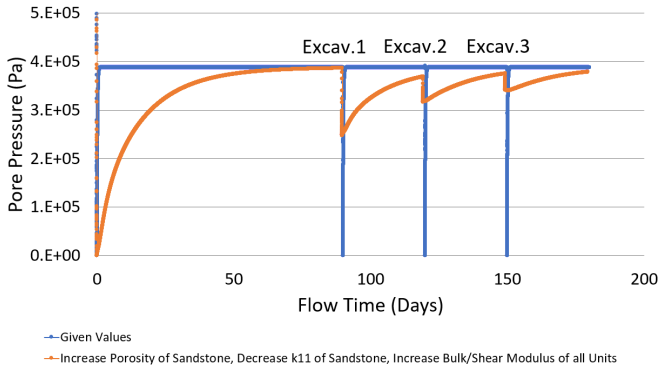

Fig. 12. Modeled pore pressure (Pa) versus groundwater flow time (days) for Model Case H (orange) and Model Case A (blue).

5. CONCLUSIONS AND FUTURE WORK

A series of 2D numerical models using *FLAC* v8.1 was analyzed using a simplified two-step coupled (undrained-drained) approach. Site data (geology, geometry, mining sequence, material properties, piezometer time series of water elevation) from a mine in Nevada was used as a base-case model. A hydromechanically-coupled model was shown to reproduce similar observed behaviors to the site piezometer data.

Parameters governing the hydromechanical response of the slope during unloading were varied for a number of case-specific model simulations. The results were analyzed to assess the sensitivity of these governing parameters to the simulated responses.

The model results showed generally:

- Increasing the stiffness of the material allowed the model to reach the initial solved equilibrium flow state quicker, as well as retaining more realistic (non-zero) pressures prior to initiation of the drained analysis stage.
- Stress relief due to excavations produced more rapid drops in pore pressure with lower rock porosity. Increasing the porosity of the material allowed the slope to retain more realistic starting pressures prior to initiation of each drained analysis stage, as well as a more gradual pore pressure recovery with initiation of flow back into the model.
- The recovery of the fluid pressure after unloading is highly sensitive to the horizontal permeability of the material when groundwater flow is primarily occurring within horizontal layers. Lower permeability results in pore pressures that do not recover as quickly from the initial pressure drop with stress relief. As well, the initialization

time to reach equilibrium flow state of the model should be extended for lower permeability material.

Overall, pore-pressure drops due to volumetric expansion of the rock mass have the potential to benefit slope performance and stability. These model results will help the practitioner determine the types of situations where hydromechanical coupling may be applicable for the design of rock slopes and which parameters are most important for governing the pore pressure behavior. Porosity is seen to be a key control on the magnitude of pressure change which is important in fracture-flow settings as most rocks exhibit low drainable porosity. Understanding the pore pressure recovery after unloading is important for helping to determine the length of time available before the pore pressures start to rebound and the effective stress of the slope materials starts to reduce.

Future work regarding this modeling effort is proposed to improve model realism through the following:

- Producing a model that is more realistic to the specific site conditions, which could include more detailed geology, geometry, mining excavation rate, spatial distribution of properties, and laboratory values for intact rock modulus.
- Extending the left model boundary and increasing the width of the model domain to investigate the sensitivity of lateral confinement and better represent the hydraulic boundary conditions.
- Incorporating additional external effects to flow that result from active site dewatering and drainage measures. The calibration data likely contains an overprint, whereas our model is fixed and just relies on permeability and porosity.
- Transitioning to a 3D model to consider wider (off-section) effects beyond the 2D space.

REFERENCES

1. Beale, G., and Read, J. (2014). Guidelines for Evaluating Water in Pit Slope Stability. CSIRO Publishing.
2. Beale, G. (2018). How our understanding of water and slope stability has improved since 2009. *Slope Stability 2018*. Seville, Spain.
3. Galera, J. M., Montero, J. and Perez, C., Montego, L. and Varona, P. (2009). Coupled Hydromechanical Analysis of Cobre Las Cruces Open Pit. In *Proc. Slope Stability 2009*, Santiago, Chile. Universidad de Los Andes.
4. Hazzard, J., Damjanac, B., Detournay, C., and Lorig, L. (2011). Developing rules of thumb for groundwater modelling in large open pit mine design. In *Proc. 2011 Pan-Am CGS Geotechnical Conference,* Toronto, Canada, Canadian Geotechnical Society.
5. Itasca Consulting Group, Inc. (2019). FLAC, Fast Lagrangian Analysis of Continua, FLAC 8.1 Reference. First Edition (FLAC Version 8.1). Minneapolis, Minnesota.
6. Sullivan, T.D. (2007). Hydromechanical Coupling and Pit Slope Movements. *Keynote Address, Slope Stability 2007*. Perth, Australia. Australian Centre for Geomechanics.
7. Terzaghi, K. (1943) “Theoretical Soil Mechanics.” Wiley, New York.